C. L

DEVIATIONS FROM INTEGRATING SPHERE THEORY CAUSED BY CENTRALLY LOCATED SAMPLES

J. P. Dawson, D. C. Todd, B. E. Wood, et al.

ARO, Inc.

April 1966

AEROSPACE ENVIRONMENTAL FACILITY
ARNOLD ENGINEERING DEVELOPMENT CENTER
AIR FORCE SYSTEMS COMMAND
ARNOLD AIR FORCE STATION, TENNESSEE

NOTICES

DEVIATIONS FROM INTEGRATING SPHERE THEORY
CAUSED BY CENTRALLY LOCATED SAMPLES

J. P. Dawson, D. C. Todd, B. E. Wood, et al.

ARO, Inc.

FOREWORD

The research reported herein was sponsored by Arnold Engineering Development Center (AEDC), Air Force Systems Command (AFSC), Arnold Air Force Station, Tennessee, under Program Element 61405014/8951.

The results of the research were obtained by ARO, Inc. (a subsidiary of Sverdrup and Parcel, Inc.), contract operator of AEDC under Contract AF 40(600)-1200. The work was done under ARO Project No. SW2407, and the manuscript was submitted for publication on November 29, 1965.

In addition to the authors listed on the cover, the report was written by B. A. McCullough, ARO, Inc., and R. C. Birkebak, Georgia Institute of Technology.

This technical report has been reviewed and is approved.

Terry L. Hershey
Captain, USAF
Aerospace Sciences Division
DCS/Research

Donald R. Eastman, Jr.
DCS/Research

ABSTRACT

A review of the assumptions made in the theory of the classical integrating sphere is given. The validity of these assumptions as applied to a modified integrating sphere is discussed in terms of a computer analysis and experimental data. The results of the analysis indicate that a possible error of 15 percent may be introduced into the absolute reflectance determinations. This can occur when the classical theory is applied to a modified integrating sphere using the angular-hemispherical technique. The parameters considered in the analysis are irradiance, sphere radius, sample reflectance, specular component of the sample, angle of incidence, and detector location.

CONTENTS

ILLUSTRATIONS

TABLE

NOMENCLATURE

A	Area of the interior sphere wall, cm^2
A_j	Area of piece "j", cm^2
D	Detector
E	Diagonal matrix of reflectances
F	Form factor matrix
F_{ij}	Form factor from i to j
F_{ikj}	Form factor from i to k to j
G_{ij}	Form surface factor
$H_{\ell j}$	Irradiance on piece j from piece ℓ, w/cm^2
I	Identity matrix
I_0	Energy, w
I_{S_1}	Incident energy on S_1, w/cm^2
I_{S_2}	Incident energy on S_2, w/cm^2
$I_{\theta,\phi}$	Incident energy at ϕ when sample is irradiated at θ, w/cm^2
$I_{\psi,\phi}$	Incident energy at ϕ when sphere wall is irradiated at ψ, w/cm^2
k	Detector constant, $mv/w/cm^2$
N	Number of pieces of sphere
P_i	Energy flux leaving piece "i", w
P_{ij}	Energy flux leaving piece "i" and incident on piece "j", w
Q_{ℓ_i}	Energy flux from piece "ℓ" to piece "i", w
R	Radius of sphere, in.
r	Radius of sample disk, in.
S	Sample surface
St	Standard sample

V	Detector output, mv
α	Specular component
β	Azimuthal angle, deg
ϵ	Incident energy
θ	Angle of incident beam on sample, deg
ρ	Reflectance
ϕ	Polar angle of reflection, deg
ψ	Polar angle of incident radiation, deg
Δw	Solid angle containing reflected radiation

SUBSCRIPTS

d	Diffuse reflecting sample
i	Piece "i"
j	Piece "j"
ℓ	Piece "ℓ"
r	Reflected
S_1	Pertaining to side 1 of sample S
S_2	Pertaining to side 2 of sample S
s	Specularly reflecting sample
st	Standard sample
w	Pertaining to interior sphere wall

SECTION I
INTRODUCTION

There are three basic types of instruments which are used to measure the reflectances of surfaces. These systems are the Coblentz hemisphere, the heated cavity reflectometer, and the integrating sphere. They were evaluated by Dunkle (Ref. 1) in a recent review paper on reflectance measurements. The hemisphere with variations has several basic problems such as critical locations of detector and sample, nonuniform detector response to both angle of incidence and image location, and optical aberrations. The heated cavity reflectometer is not operable in the visible range unless very high temperatures are maintained in the cavity. This is caused by large errors which are introduced by small temperature gradients in the heated cavity. Of these systems, the integrating sphere is capable of the most precise measurements over the largest wavelength range if a few precautions are taken about the choice of sphere wall materials and the location of sample, detector, and entrance port.

The integrating sphere has been used to determine the reflectance of various surfaces for many years, and extensive literature exists describing its applications. Several investigators have analyzed the theory of the integrating sphere (Refs. 2 through 5). They have considered the case of a perfect sphere where the area of the apertures for illumination and viewing as well as the sample port are negligible compared to the area of the sphere. Hardy and Pineo (Ref. 6) discussed the errors caused by the finite size of the apertures, but they considered only the photometric method and did not mention the mathematical techniques used. The effects of finite apertures on the reflectance were also treated by Preston (Ref. 7); however, his method cannot be easily extended to more general cases.

Since the theory of the integrating sphere is the theory of multiple reflections in a confined system, this problem of interreflection can be formulated as an integral equation. Moon (Ref. 8) gave a discussion of this considering the apertures to be negligibly small. Jacquez and Kuppenheim (Ref. 9) extended Moon's work and derived an integral equation which considers the aperture sizes, geometry of the sample and standard, and the effects of a specular component on the reflectance measurements. All of these discussions assumed perfect sphere, perfectly diffuse reflections from the wall, and that the wall was uniformly irradiated. Also, the sample and standard were located on the wall of the sphere. When the sample is on the wall, the angle of incidence of the

1

light beam is governed by the size of the sphere and the geometry of the entrance aperture. In most cases the angle of incidence is 5 to 15 deg from the sample normal.

The need for reflectance measurements (Refs. 10 and 11) as a function of angle of incidence of the light beam has led to modifications in the standard integrating sphere. The most common modification is to place the sample in the center of the sphere and to rotate the sample to obtain the desired angle of incidence. Such systems have been described by Edwards (Ref. 11), Wood (Ref. 12), and Birkebak (Ref. 13). This location of the sample alters the distribution of the reflected radiation within the sphere and, therefore, the sphere walls are not uniformly irradiated as is assumed in the classical theory. The purpose of this report is to formulate the general problem of the integrating sphere with the sample in the center and to determine the effect of the center sample on the wall irradiance and on the calculation of sample reflectance.

SECTION II
CLASSICAL INTEGRATING SPHERE THEORY

The reflectance of a surface is normally defined as the ratio of reflected to incident radiation. Previous investigators have shown that the reflectance is a function of surface material, radiation wavelength, angle of the incident radiation, and surface roughness. For the following discussion the surface material, the wavelength, and the surface roughness will be held constant. It is assumed that the interior walls of the spheres are diffuse reflectors with a reflectance, ρ_w, of 96 percent, and that the detector is a perfect absorber.

The classical or perfect integrating sphere (Fig. 1), as discussed by Jacquez and Kuppenheim (Ref. 9), is considered to be a sphere with negligible size apertures whose walls are uniformly irradiated by multiple reflections. The sample, S, and the standard, St, are curved such that they continue the sphere wall and, therefore, no correction need be applied for flat surfaces.

When radiation, I_o, is incident on the diffusely reflecting sample, the reflected radiation is $\rho_d I_o$, ρ_d being the reflectance of the sample. The irradiance of any unit area on the sphere wall from this reflection would be $\rho_d I_o / A$. Then the detector response from the first reflection would be given by

$$V_1 = k \rho_d I_o / A \qquad (1)$$

From the second reflection, the radiation striking the detector would be $(\rho_w \rho_d I_o)/A^2$ from each unit area or summing over all unit areas the detector response would be

$$V_2 = k \frac{\rho_w \rho_d I_o}{A} \tag{2}$$

From the third reflection

$$V_3 = k \frac{\rho_w^2 \rho_d I_o}{A} \tag{3}$$

Summing over all reflections, the total detector response would be

$$V_d = \sum_1^\infty V_i = k \frac{\rho_d I_o}{A} (1 + \rho_w + \rho_w^2 + \rho_w^3 + \cdots) \tag{4}$$

or in closed form

$$V_d = k \frac{\rho_d I_o}{A} \left(\frac{1}{1 - \rho_w} \right) \tag{5}$$

Applying the same method to the standard sample yields a detector response of

$$V_{st} = k \frac{\rho_{st} I_o}{A} \left(\frac{1}{1 - \rho_w} \right) \tag{6}$$

and the ratio of Eq. (5) to Eq. (6) gives the equation of Jacquez and Kuppenheim (Ref. 9)

$$\frac{\rho_d}{\rho_{st}} = \frac{V_d}{V_{st}} \tag{7}$$

This equation has been used by many investigators for calculating ρ_d. However, if the sample is not a perfectly diffuse reflector, this equation is not accurate. To illustrate this, the same sphere with a perfectly specular reflecting sample is considered. The detector does not see the first reflection because of the specular reflection from the sample. Therefore, $V_1 = 0$, and the detector response from the second reflection would be

$$V_2 = k \frac{\rho_w \rho_s I_o}{A} \tag{8}$$

From the third

$$V_3 = k \frac{\rho_w^2 \rho_s I_o}{A} \tag{9}$$

Summing over all reflections, the total detector response for the specular sample would be

$$V_s = \sum_1^\infty V_i = k \left[0 + \frac{\rho_w \rho_s I_o}{A} + \frac{\rho_w^2 \rho_s I_o}{A} + \cdots + \frac{\rho_w^{N-1} \rho_s I_o}{A} \right] \tag{10}$$

or in closed form

$$V_s = k \ \frac{\rho_w \rho_s I_o}{A} \left(\frac{1}{1 - \rho_w} \right) = k \ \frac{\rho_s I_o}{A} \left(\frac{\rho_w}{1 - \rho_w} \right) \qquad (11)$$

and since $\rho_w = \rho_{st}$

$$\rho_s = \frac{V_s}{V_{st}} \qquad (11a)$$

The detector response for a diffuse sample (Eq. (5)) and a specular sample (Eq. (11)) are different by a factor of ρ_w. Jacquez and Kuppenheim (Ref. 9) arrive at the same general equation through a more rigorous mathematical treatment. These equations show that if a sample has both a diffuse and a specular component neither equation will give an accurate value for the reflectance, the greatest error being $1 - \rho_w$.

SECTION III
MODIFIED SPHERE, ANGULAR-HEMISPHERICAL TECHNIQUE

The most common modification to the classical integrating sphere has been the placement of the sample in the center of the sphere (Fig. 2). For example, a case where the angular-hemispherical technique (Fig. 2) is employed will be considered. Radiation strikes the test surface at some given angle, θ, and is reflected into the top hemisphere. For this system, where the sample is located in the center of the sphere, the assumption of equal irradiance on the wall is not valid. This can be shown by considering the first reflection of incident radiation from the sample.

If the sample is a perfectly diffuse reflector, the distribution of the radiation reflected into the top hemisphere will follow the cosine law. Then the area of wall normal to the sample surface will have the highest irradiance, and the irradiance will decrease as a cosine function (Fig. 2). The bottom hemisphere being shadowed by the sample will not be irradiated by the first reflection. For subsequent reflections, all areas of the sphere wall will be irradiated. However, the shadowing effect of the sample must be considered for precise calculations. Calculation of wall irradiance requires a computer because each form factor and form surface factor must be obtained for each unit area, and for the desired accuracy a large number of terms must be used in the series in Eq. (4). Such a computer program has been written, and the mathematical method used in the program is discussed in the next section.

The case of the perfect specular reflecting sample is less complicated than that of the diffuse reflector. The radiation is incident on the sample at some angle θ and is specularly reflected at the angle ϕ, where $\theta = \phi$. Only a small area is irradiated by the first reflection, and this area is normally quite small compared to the total sphere wall area. Neglecting this small area, the equation derived for the specular sample (Eq. (11)) can be used to calculate the reflectance of the center sample. However, the shadow effect again has been neglected.

SECTION IV
MATHEMATICAL METHOD

Consider a modified sphere (Fig. 3) which is of radius R and has a diffuse reflecting interior surface with reflectance ρ_w. The centrally located sample is considered to be an infinitely thin disk of radius r, and the system is symmetrical about the z-axis. Divide the sphere into N pieces (Fig. 3), determined by planes perpendicular to the z-axis, and label them from 1 to N. Let the test surface of the sample, S_1, be piece N + 1 and the other side, S_2, be piece N + 2 with their respective specular components being a_1 and a_2.

For case 1, assume that $a_1 = a_2 = 0$ If energy of flux P_i leaves piece i diffusely and uniformly and then, considering all reflections, there will be a resulting flux P_{ij} on piece j. Since P_{ij} is directly proportional to P_i, a form surface factor can be defined as

$$G_{ij} = P_{ij}/P_i \tag{12}$$

which will depend only on the nature of surface and the geometrical configuration of the system.

It is shown in Appendix I that by making the pieces small enough, that G is approximated by an infinite series of matrices involving only the form factor matrix, F, and the diagonal matrix of the reflectances, E. It is also shown that

$$G = F (I - EF)^{-1} \tag{13}$$

Thus, G may be calculated by summing a series or by inverting a matrix. The first method was used in this report because better accuracy was obtained.

Let a collimated beam of flux $Q_{\ell i}$ from a source on piece ℓ be incident on piece j. Then flux

$$P_i = \rho_i Q_{\ell i} \tag{14}$$

will leave piece i diffusely (and it will be assumed uniformly) so that P_{ij} can be calculated from Eq. (12). The irradiance $H_{\ell j}$ incident on piece j, resulting from $Q_{\ell i}$, is found by dividing P_{ij} by the area, A_j, of piece j. This results in

$$H_{\ell j} = \frac{\rho_i Q_{\ell i} G_{ij}}{A_j} \tag{15}$$

For case 2, assume that of the flux reflected from S_k ($k = 1, 2$) that a_k is reflected specularly and that ($1 - a_k$) is reflected diffusely. Now consider flux leaving piece i. Depending on the location, a fraction, f_{ikj}, of this flux will be reflected specularly from S_k onto piece j. It is shown in Ref. 14 that

$$f_{ikj} = a_k \rho_{n+k} F_{ikj} \tag{16}$$

where F_{ikj} is the form factor from piece i to the part of the image of piece j reflected in the plane of the disk, which can be seen through S_k.

Now define a new "form factor" F' by

$$F'_{ij} = F_{ij} + f_{i_1 j} + f_{i_2 j} \tag{17}$$

Also, since only ($1 - a_k$) of the flux leaving S_k, leaves diffusely let

$$F'_{n+k, j} = (1 - a_k) F_{n+k, j} \tag{18}$$

In this case F' is used instead of F when calculating G.

As before, the irradiation resulting from $Q_{\ell i}$, where $i \leq n$, is given by Eq. (15). However, consider the radiation from $P_{\ell, n+k}$. An amount, $\rho_{n+k} (1 - a_k) Q_{\ell, n+k}$, will leave S_k diffusely. The factor of ($1 - a_k$) has already been considered by altering the form factors according to Eq. (18). Also, an amount, $\rho_\ell \rho_{n+k} a_k P'_{\ell i}$, will be leaving piece ℓ diffusely. In actuality this flux will be leaving an area the same size as the area of the source. It will be assumed that it leaves piece ℓ uniformly. Although this is only an approximation to the actual condition, if we consider that the flux is leaving diffusely and will be diffusely reflected many times, the assumption leads to a good approximation. With this assumption it can be shown that the irradiation on piece j resulting from $Q_{\ell, n+k}$ is

$$H_{\ell j} = \frac{\rho_{n+k} Q_{\ell, n+k} (G_{n+k, j} + \rho_\ell a_k G_{\ell, j})}{A_j} \tag{19}$$

The method of this analysis is based on Eq. (19). It is seen from Eqs. (16), through (19) that case 2 reduces to case 1 when $a_k = 0$.

SECTION V
RESULTS

With the aid of the computer program, the wall irradiance was calculated as a function of ρ_{S_1}, ρ_{S_2}, α_1, α_2, θ, ϕ, ψ, and R/r. These quantities are identified in Fig. 4. Also, the reflectance of each test sample was calculated, employing Eqs. (7) and (11a), to determine the error caused by unequal wall irradiance. Experimental data were obtained on similar samples in a 7-in. integrating sphere for comparison purposes. These results are presented graphically and are discussed in the next section. These results are based on a sphere which has been divided into 16 parts, and a sufficient number of reflections were considered to give an accuracy of 0.01 percent in the wall irradiance. The values of I_ϕ given are the averages of the sphere piece considered, and ϕ is equal to the angle which designates the midpoint of the piece.

SECTION VI
DISCUSSION

6.1 ANGULAR-HEMISPHERICAL TECHNIQUE

The system parameters used in this discussion are illustrated in Fig. 4. When the angular-hemispherical technique is used, the radiation, ϵ_i, strikes the test surface S_1, at an angle θ measured from the surface normal, and the irradiance on the wall is given in terms of the angle ϕ. For the graphs shown, $\theta = 5.6$ deg unless otherwise stated.

Consider a diffuse reflecting sample which has a reflectance of 5 percent $(\rho_{S_1}, \rho_{S_2} = 0.05; \alpha_1 = \alpha_2 = 0)$. The irradiance of the sample is 0.7 in. and is kept constant for all calculations. The irradiance on the wall is given in Fig. 5 as a function of ϕ for integrating spheres with radii of 3.5, 5, 6, and 7 in. The radius of the sample is 0.7 in. and is kept constant for all calculations in this report. The curves indicate that the irradiance decreases as $\cos \phi$ from $\phi = 0$ deg to $\phi = 90$ deg, but from $\phi = 90$ deg to $\phi = 180$ deg the irradiance is essentially constant. If each reflection is considered individually, this is the expected result. Since the first reflection has a diffuse distribution (Fig. 4), a, the area normal to the surface ($\phi = 0$ deg) would have the higher irradiance and the irradiance would decrease to zero at $\phi = 90$ deg. The lower hemisphere would not be irradiated by the first reflection. However, for each subsequent reflection the sphere wall would be equally irradiated by each reflection because of the diffuse reflecting wall. This is subject

to a correction for the shadowing effect of the sample. The change in irradiance between the various spheres is caused by the increase in actual interior surface area of the integrating spheres and the R/r ratio. The percentage difference in irradiance between the upper and lower hemispheres is the same in each case. That is, if the irradiance was normalized for the various sphere radii one would obtain a single curve. Also, since the sample was assumed to be a perfectly diffuse reflector, the same curves are obtained when θ is varied from 0 to 90 deg. To compare the perfectly specular reflecting surface with the perfectly diffuse, the dashed curves in Fig. 5 show the wall irradiance on spheres with 3.5- and 6.0-in. radii. All other parameters are the same except that now $\alpha = 1$.

Now consider the case where the radiation strikes the wall first. The area which is illuminated by the incoming radiation is determined by the angle ψ, measured from the normal to S_2 (Fig. 4). The change in irradiance of the wall under these conditions varied less than 1.0 percent from $\phi = 0$ deg to $\phi = 180$ deg. This variation was caused primarily by the absorption of radiation by S_2. This observation is shown in Fig. 6 for three sphere sizes. The irradiance on S_2 is plotted versus the angle ψ. When the area normal to S_2 is irradiated, the irradiance on S_2 is the greatest and as ψ increases to 90 deg the irradiance decreases as a function of the cos ψ. This is caused by the decrease in area of S_2 (form surface factor) as seen by the radiating area of the sphere wall. Thus, less radiation from the first reflection is absorbed by S_2, and a slightly higher irradiance is observed at $\psi = 90$ deg. The dotted line is the irradiance on S_1 and as shown, $I_{S_1} = I_{S_2}$ when the radiating surface is 90 deg from the normals of the two surfaces. The circular points on the curve for the 3.5-in. radius sphere are experimental points measured by substituting solar cells for S_1 and S_2. The data have been normalized with respect to the I_{S_2}, $\psi = 25$ deg.

The following equation was used to calculate the reflectance of S_1, ρ_{S_1}, from these data.

$$\rho_{S_1} = \rho_w \frac{I_{\theta,\phi}}{I_{\psi,\phi}} \tag{20}$$

Where ρ_w is the reflectance of the wall; $I_{\theta,\phi}$ is the irradiance at ϕ when the sample is irradiated at θ; $I_{\psi,\phi}$ is the irradiance at ϕ when the incident radiation strikes the wall at ψ. Since S_1 is a diffuse reflecting sample, $I_{\theta,\phi}$ will be a constant when θ varies from 0 to 90 deg, and it has been stated that $I_{\psi,\phi}$ varied less than 1 percent for all angles of ψ and ϕ. To analyze the effects of the parameters on reflectance measurements, all the calculations are for $\theta = 5.6$ deg and $\psi = 61.9$ deg.

Using Eq. (20) or its equivalent, Eq. (7), and $I_{61.9}$, ρ_{S_1} was calculated for each value of ϕ for spheres of radius 3.5, 5, and 7 in. In Fig. 7, these results are compared to ρ_{S_1} calculated assuming equal wall irradiance. The reflectance of a sample is usually measured with the detector located at $\phi = 90$ deg; this is indicated on the figure by an arrow. As is shown by the curves, if the reflectance of a sample is measured with the detector at the indicated point, the value of the reflectance will be in error. Several investigators have made reflectance measurements with such systems, have compared their results with other published data, and have reported good agreement with spheres of different sizes. However, the curves (Fig. 7) show that with the detector located at ϕ near 90 deg, the spheres would give essentially the same result and it would be in error by approximately 4 percent. The circular points on the figure are experimental data obtained with a 3.5-in. radius sphere. These data have been normalized with respect to $\phi = 80$ deg.

In Fig. 8, ρ_{S_1} calculated from Eq. (7) is compared to that expected when the sphere wall irradiance does not vary (solid lines). The error in the measurement caused by unequal irradiance is shown in Fig. 9 for values of ρ_{S_1} from 5.0 to 100 percent for various size spheres. The values of θ, ψ, and ϕ are as indicated in the figure. The absolute error is shown in Fig. 10 as a function of R and ρ_{S_1}. The absolute error is shown again in Fig. 11 to illustrate the change in error as a function of R/r for different values of ρ_{S_1}.

Another factor which influences the irradiance is the reflectance of the back side of the test surface, ρ_{S_2} (Fig. 12). Although the general shape of the distribution curve is not changed, the curve is shifted as ρ_{S_2} varies from 0 to 1.0 as shown by Fig. 12. If the reflectance measurements are obtained with the detector at $\phi = 90$ deg, the greatest error introduced by S_2 is 2.0 percent.

In precise calculations, the effect of the specular component of the test sample must also be considered. One would not expect the specular component, a_2, of S_2 to have much influence on the wall irradiance since the sample is essentially irradiated equally from all angles, and the distribution of the reflected light would not vary much if the sample were diffuse or specular. However, the specular component, a_1, of S_1 is of vital importance when using the angular-hemispherical technique. Since the incoming radiation is incident on the sample, the distribution of the radiation on the top hemisphere is dictated by a_1 and the angle of incidence, θ. Figure 13 shows the effect of a_1 on ρ_{S_1} calculated from the classical sphere equations. The curve for $a_1 = 0$ was calculated using the equation for a diffuse sample, Eq. (7), and the curve for $a_1 = 1.0$

from Eq. (11a). The curves for the other values of a_i were obtained from the following equation.

$$\rho_{S_i} = (1 - a_i) \frac{I_{\theta,\phi}}{I_{\psi,\phi}} (\rho_w) + a_i \frac{I_{\theta,\phi}}{I_{\psi,\phi}} \qquad (21)$$

This equation implies that the specular and diffuse components are completely separable and that no interaction occurs. The validity of this assumption is dependent on the particular surface being tested. Measurements of the distribution of light reflected from some metal samples have shown that the specular component could be treated separately; that is, the specular component was a sharp spike super-imposed on a diffuse or spherical distribution. However, other samples have shown that the two components are inseparable because the distribution is oval.

The absolute error in the determination of ρ_{S_i} caused by using the classical sphere equations for the calculation are shown in Fig. 14 for several sphere sizes. The largest error occurs when $a_i = 0$ and the smallest when $a_i = 1.0$. The curve connecting these two points was determined by Eq. (21) and is subject to the assumptions previously stated.

Several investigators have stated that if the angular-hemispherical technique is used and the detector does not see the first reflection from the sample, Eq. (11a) will give the correct value of ρ_{S_i}. Although it is true that the value of ρ_{S_i} calculated from Eq. (11a) when $\phi = 90$ deg is in better agreement with the true value of ρ_{S_i} than the value obtained from Eq. (7), the reason given for using the equation is not valid. This is shown in Fig. 15. The solid line represents the value of ρ_{S_i} obtained from a perfect sphere as a function of ϕ for $a_i = 0$ or 1.0. Curve number 3 shows ρ_{S_i} as a function of ϕ calculated from Eq. (11a) for a sample, $a_i = 1.0$, in a modified sphere. Curve number 2, calculated from Eq. (7), is for a diffuse sample. As indicated, curve number 1, calculated from Eq. (11a) with $a_i = 0$, gives a more accurate value of ρ_{S_i} at $\phi = 90$ deg but it is purely fortuitous. This can be shown by considering the total energy in the system. If a sample, $\rho_{S_i} = 0.05$, is irradiated by a source with I_0 watts then the energy reflected is 0.05 I_0 watts. This energy is dis-tributed throughout the sphere and in the perfect sphere case, the total energy is proportional to the area under the curve for the perfect sphere. The area under curve number 3 is proportional to the energy for the $a_i = 1.0$ case. This total area is approximately 4 percent less than that for the perfect sphere. This is to be expected since the detector does not see the first reflection from the sample, and its reading would be re-duced by ρ_w. The area under the second curve is 0.4 percent less than for the perfect sphere, and the difference is attributable to the absorptance

of S_2. The area under curve number 1 is 2.8 percent greater than the perfect sphere case. This is not possible since it would require an addition of energy to the system. Even though the use of Eq. (11a) to calculate ρ_{S_1} gives a more accurate value under these conditions, it has no theoretical justification.

Table I shows the absolute error in the reflectance measurement when the angular-hemispherical technique is used. These data are for a 3.5-in. radius sphere with samples of various reflectances as indicated in columns I and II. The values listed in columns III, IV, and V were determined by the difference in the known ρ_{S_1} and the calculated values. The calculated values for column III were determined from Eq. (7) for ϕ = 90 deg and θ = 5.6 deg. The calculated values used to obtain the errors listed in columns IV and V were determined from Eq. (11a) for θ = 5.6, ϕ = 95 and θ = 5.6, ϕ = 130, respectively. The values for ρ_{S_1} = 0.96 are experimental points obtained with a MgO sample. The errors shown in columns III, IV, and V indicate that the classical theory of the integrating sphere does not represent the data obtained with a modified sphere. It is also apparent from these errors that the location of the detector is very critical.

6.2 HEMISPHERICAL-ANGULAR TECHNIQUE

Another measurement technique which may be used with a modified sphere is shown in Fig. 16. In this technique the radiation enters the sphere diffusely at ψ = 90 deg, and the sample is irradiated by reflections from the top hemisphere. The radiation, $I_{r\phi}$, reflected from the sample, contained in solid angle Δw_r is measured as a function of ϕ. The radiation incident on S_1, I_{ha}, is determined by viewing the radiation reflected by the sphere wall into the same solid angle, Δw_r. The sample reflectance is then determined from Eq. (11a). A detailed discussion of this technique is given in the literature (Refs. 11 and 13). The greatest change in wall irradiance as ϕ = 0 → 180 deg was less than 0.3 percent and occurred when $\rho_{S_1} = \rho_{S_2}$ = 0.05. This variance is caused primarily by the shadow effect of the sample.

A comparison of absolute, calculated, and measured reflectances for a center sample in a 3.5-in. radius sphere indicated a variation of only 0.1 percent; that is, the data would follow the dotted lines shown in Fig. 8. This implies that the assumptions and equations for the classical integrating sphere theory are valid for this technique and that accurate results can be obtained with their use.

SECTION VII
CONCLUSIONS

Calculations and experimental data have shown that the assumptions made in the classical theory of the integrating sphere are not valid for an integrating sphere with a centrally located sample when the angular-hemispherical technique is used. The error introduced by unequal wall irradiance could be as great as 15 percent depending on the reflectance of the sample and the location of the detector. The parameters ρ_{S_2}, a, and the view factors may introduce errors of 1 to 2 percent; the overall average error in absolute measurements would be about 4 percent.

The theory and assumptions for an integrating sphere, either classical or modified, were found to be valid when the hemispherical-angular technique was used. If the angular-hemispherical technique is used with a modified sphere, the system should be calibrated with a standard sample for each set of experimental conditions.

APPENDIX I

From Eq. (12), if P_i is 1 then $G_{ij} = P_{ij}$. Therefore, let a flux of unit magnitude leave piece i diffusely and uniformly. Let P_{ij}^M be the flux incident on piece j which has been reflected exactly M times, then, since flux of unit magnitude leaving i is assumed

$$P_{ij}^o = F_{ij} \qquad (I-1)$$

If it is assumed that the flux is redistributed uniformly over a piece before being reflected (this is a good assumption if the pieces are small) then

$$P_{ij}^M = \sum_{\ell=1}^{N+2} \rho_\ell \, P_{i\ell}^{M-1} \, F_{\ell j} \qquad (I-2)$$

Clearly the matrix equation is

$$P^M = \begin{cases} F & M = 0 \\ P^{M-1} \, EF & M > 0 \end{cases} \qquad (I-3)$$

Also

$$G = \sum_{M=0}^{\infty} P^M \qquad (I-4)$$

Substituting into Eq. (I-4) and simplifying one obtains Eq. (I-3)

$$G = F + \left(\sum_{M=0}^{\infty} P^M \right) EF \qquad (I-5)$$

or

$$G = F + G \, EF \qquad (I-6)$$

Solving this equation for G one obtains the result

$$G = F \, (I - EF)^{-1} \qquad (I-7)$$

Thus, one can calculate G by inverting the matrix. A more complete discussion of this method is given in Ref. 15.

REFERENCES

1. Dunkle, R. V. "Spectral Reflectance Measurements." Surface Effects on Spacecraft Materials, New York, F. J. Clauss, (ed.) John Wiley and Sons, Inc., 1960.

2. Walsh, J. W. T. Photometry. 2nd Ed., Constable and Co., Ltd., London, 1953.

3. Karrer, E. Science Papers, U. S. National Bureau of Standards, No. 415, 1921, pp. 203-225.

4. McNicholas, H. J. U. S. National Bureau of Standards, Journal of Research, Vol. 1, 1928, p. 29.

5. Rosa, E. B. and Taylor, A. H. Science Papers, U. S. National Bureau of Standards, No. 447, 1922, p. 281.

6. Hardy, A. C. and Pineo, O. W. "The Errors Due to the Finite Size of Holes and Sample in Integrating Spheres." Journal of the Optical Society of America, Vol. 21, 1931, p. 502.

7. Preston, J. S. Transactions of the Optical Society of London, Vol. 31, 1929-30, p. 15.

8. Moon, P. "On Interreflections." Journal of the Optical Society of America, Vol. 30, 1940, p. 195.

9. Jacquez, J. A. and Kuppenheim, H. F. "Theory of Integrating Sphere." Journal of the Optical Society of America, Vol. 45, 1955, p. 460.

10. McCullough, B. A., Wood, B. E., and Dawson, J. P. "Thermal Radiative Properties of Carbon Dioxide Cryodeposits from 0.5 to 1.1 Microns." AEDC-TR-65-94 (AD 468632), August 1965.

11. Edwards, D. K., et al. Journal of Applied Optics, Vol. 51, 1961, p. 1279.

12. Wood, B. E., McCullough, B. A., and Dawson, J. P. "Vacuum Integrating Spheres for Measuring Cryodeposit Reflectances from 0.35 to 15 Microns." AEDC-TR-65-178 (AD 468608), August 1965.

13. Birkebak, R. C. and Eckert, E. R. G. "Effects of Roughness of Metal Surfaces on Angular Distribution of Monochromatic Reflected Radiation." Journal of Heat Transfer, Vol. 87, February 1965.

14. Eckert, E. R. G. and Sparrow, E. M. "Radiative Heat Transfer between Surfaces with Specular Reflections." Journal of Heat and Mass Transfer, Vol. 3, 1961, pp. 42-45.

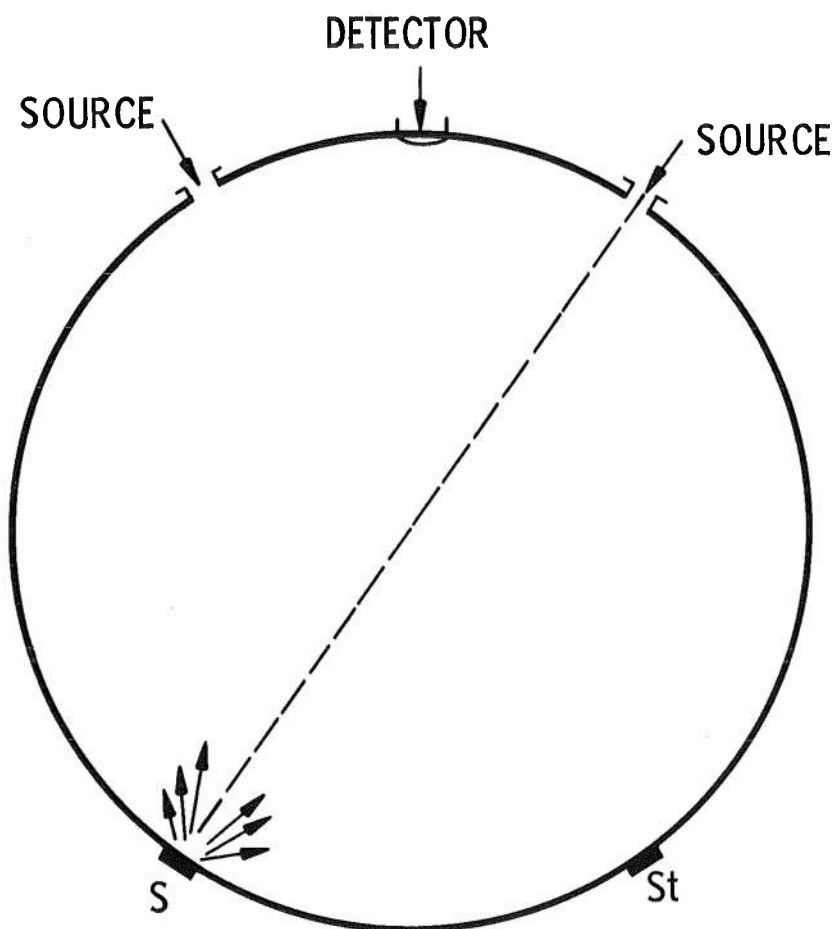15. Link, C. H. "Molecular Kinetics Studies." AEDC-TDR-63-120, August 1963.

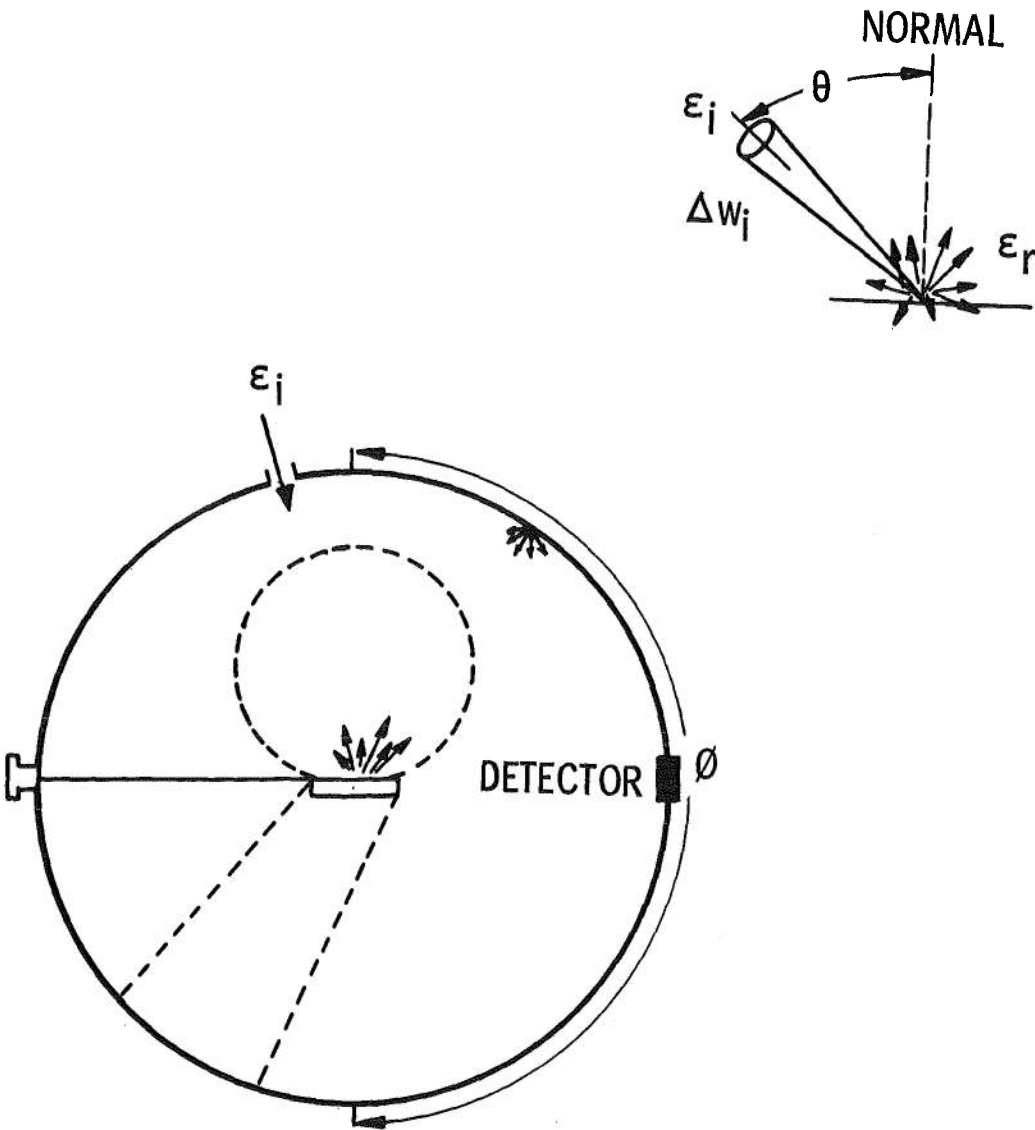**Fig. 1 Classical Integrating Sphere**
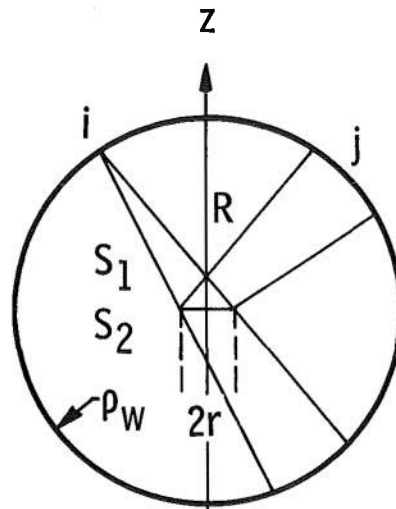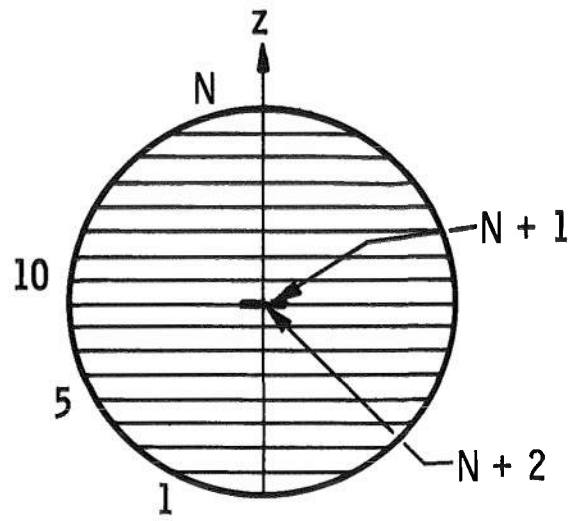
Fig. 2 Modified Integrating Sphere

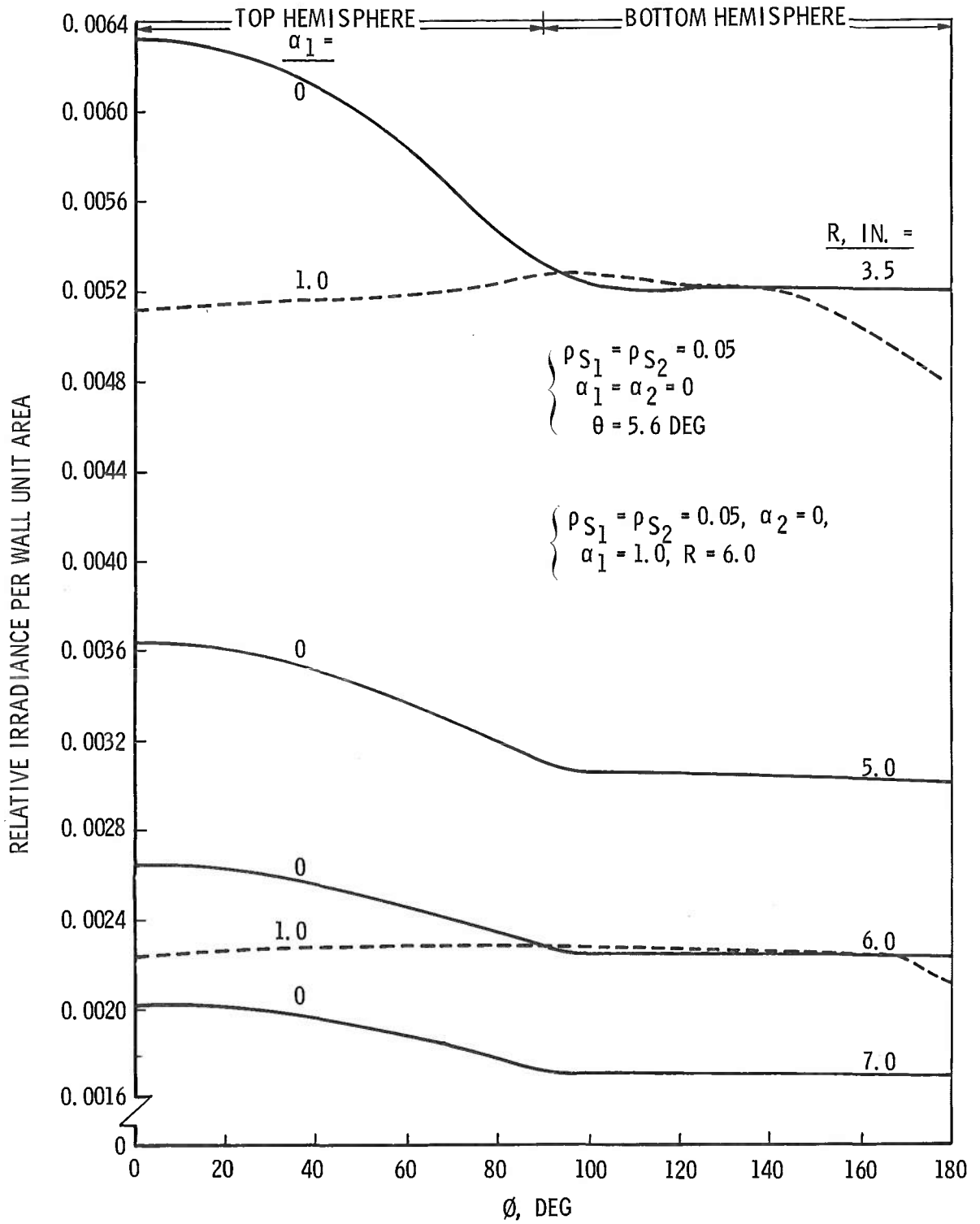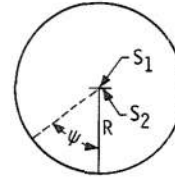Fig. 3 Mathematical Model of Integrating Sphere
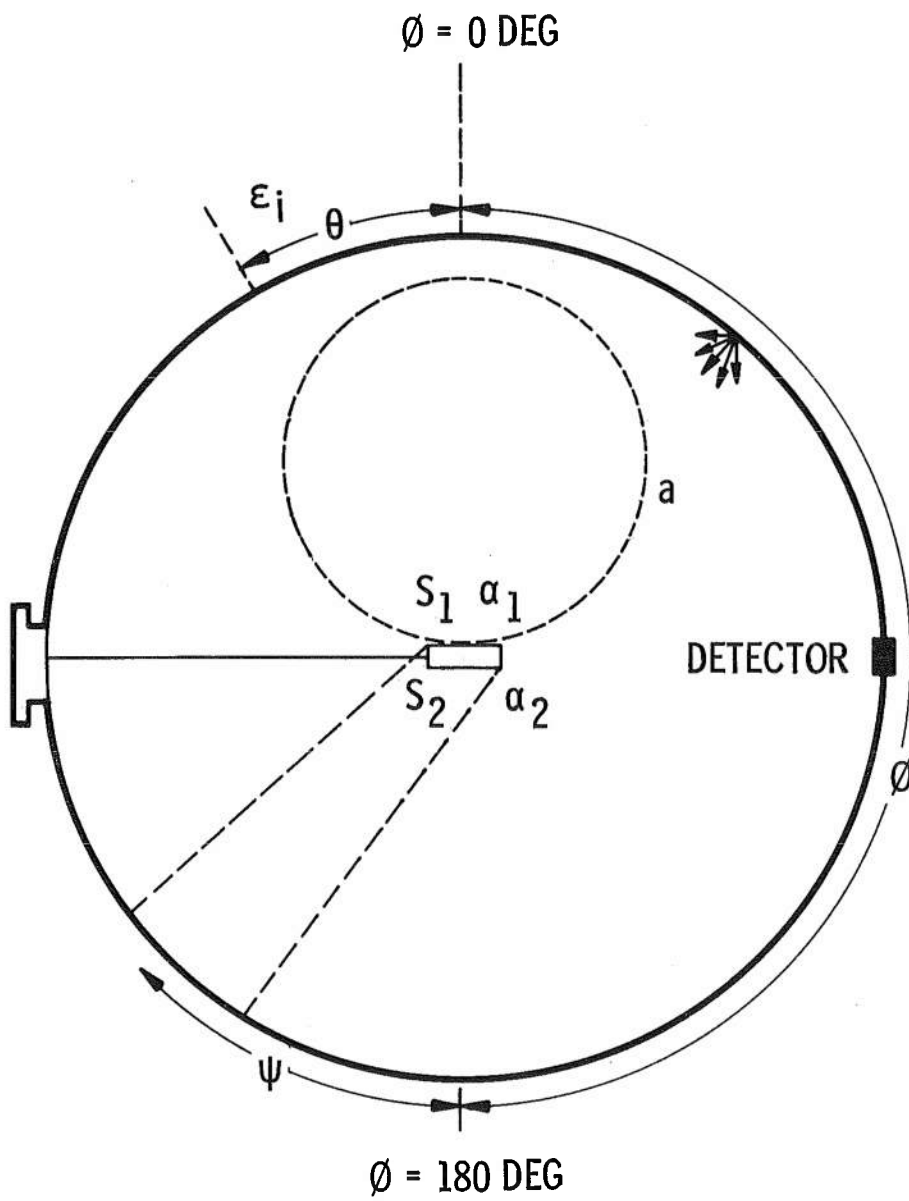
Fig. 4 Sphere Parameters

Fig. 5 Irradiance Distribution

$\rho_{S_1} = \rho_{S_2} = 0.05$
$\alpha_1 = \alpha_2 = 0$
$\psi = $ ANGLE INPUT
EXPERIMENTAL

––––––––– I_{S_1}

—————— I_{S_2}

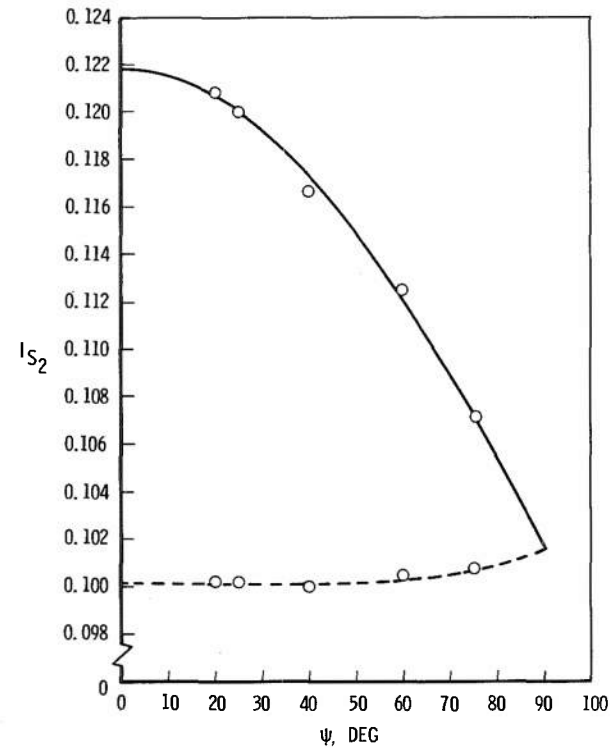SHOWS THAT CHANGE IN IRRADIANCE ON S_2 AS
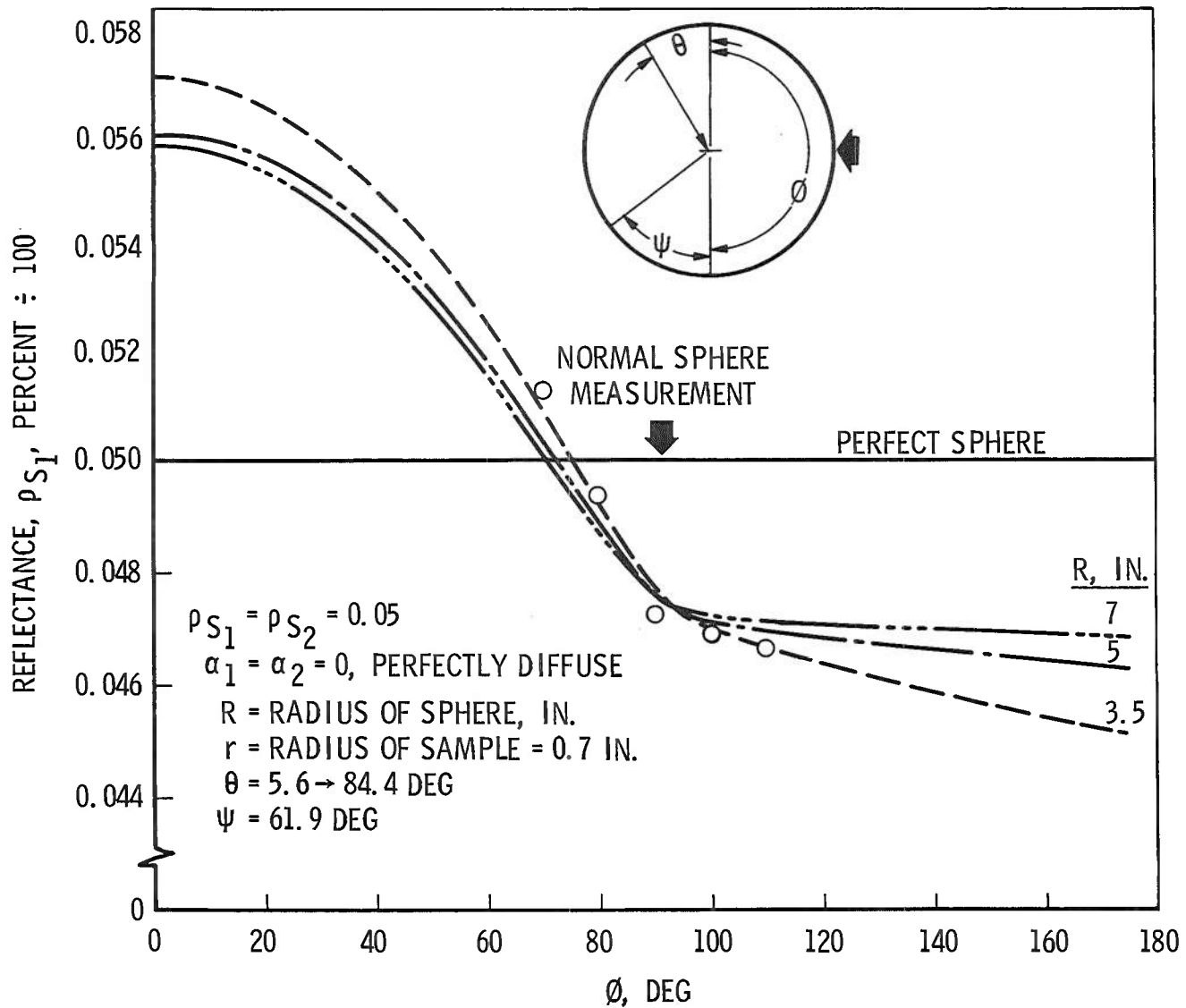$\psi = 0 \to 90$ FOLLOWS COSINE DISTRIBUTION.
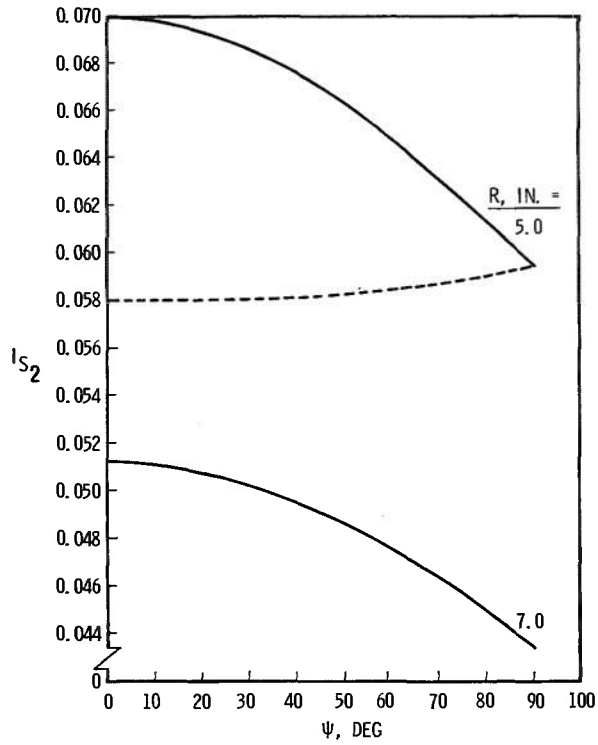
Fig. 6 Irradiance on Center Sample

Fig. 7 Reflectance as a Function of ϕ and R
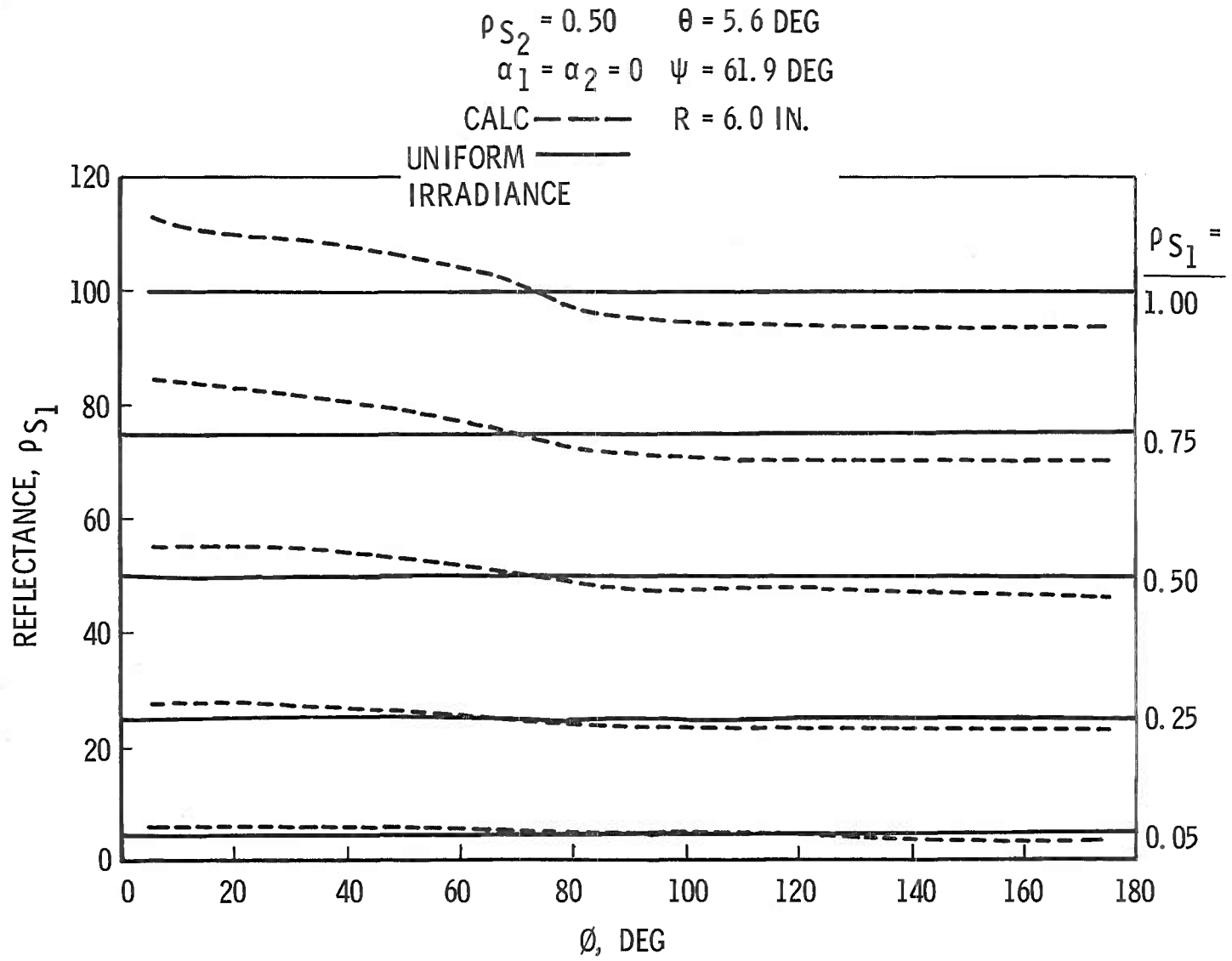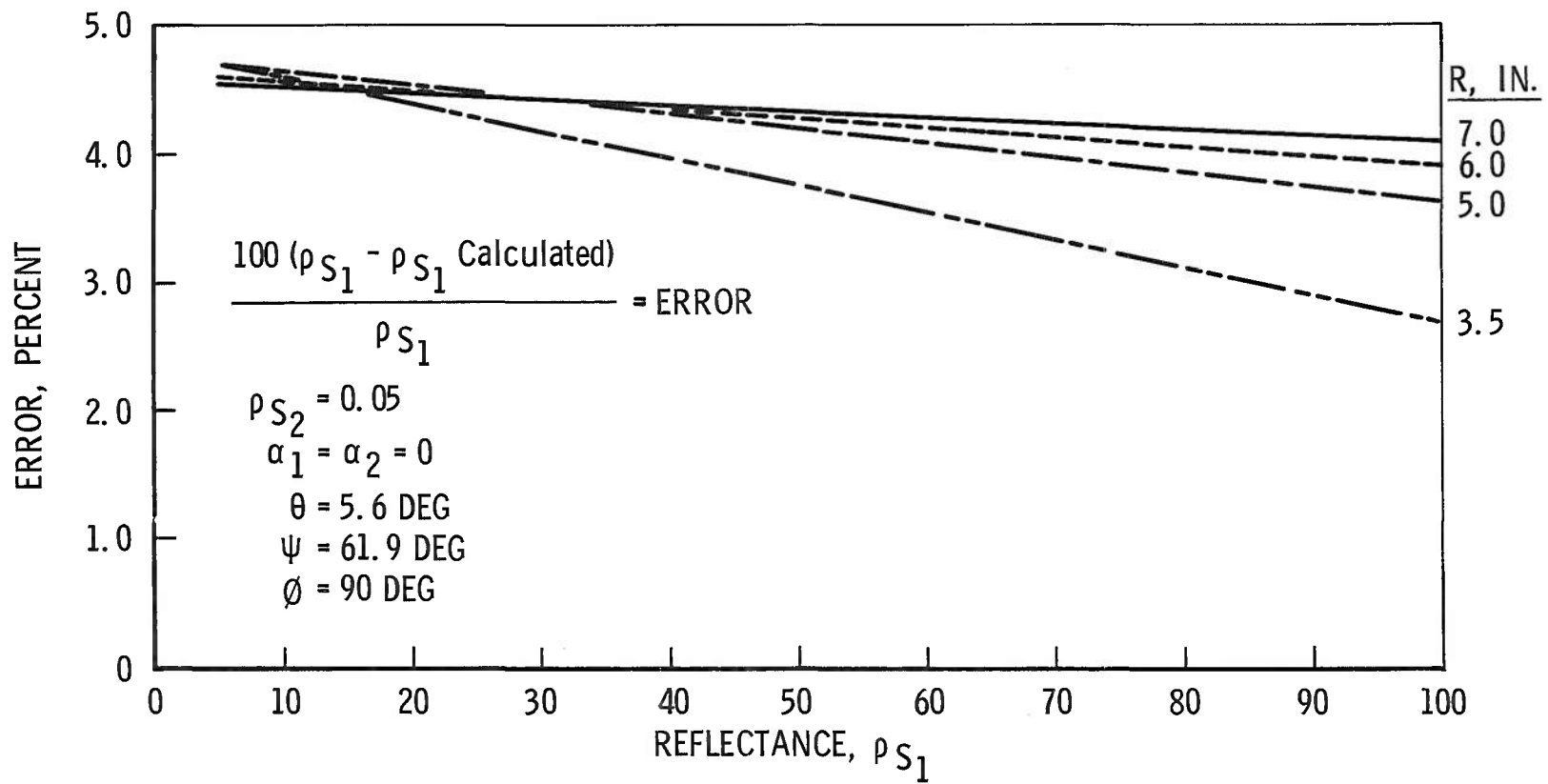
Fig. 8 Reflectance as a Function of ϕ and ρ_{S_1}
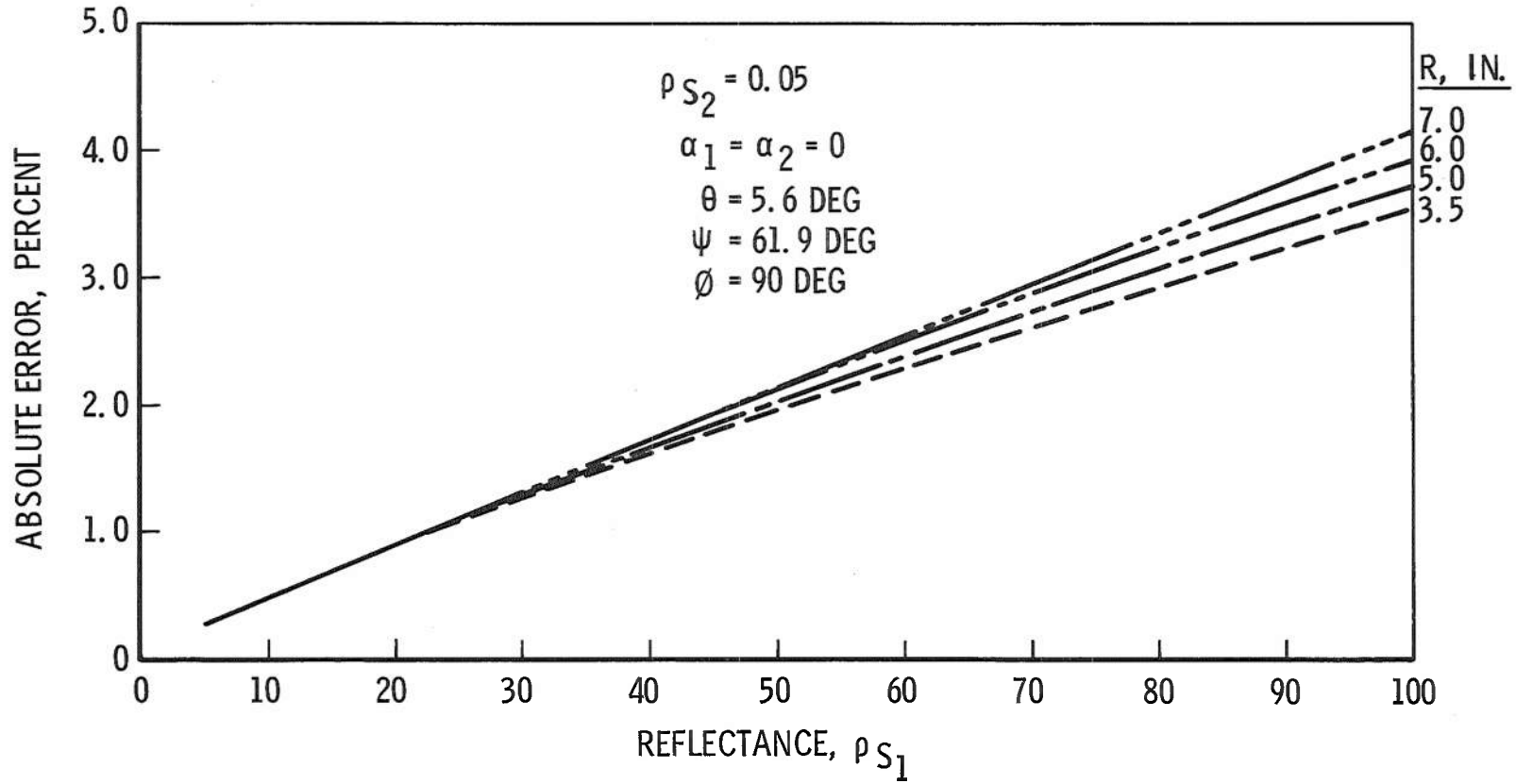
Fig. 9 Experimental Error as a Function of R and ρ_{S_1}

Fig. 10 Absolute Error as a Function of R and ρ_{S_1}

R = RADIUS OF SPHERE, IN.
$\alpha_1 = \alpha_2 = 0$
$\rho_{S_2} = 0.05$
$\theta = 5.6 \rightarrow 84.4$ DEG
$\psi = 61.9$ DEG
$\emptyset = 90$ DEG
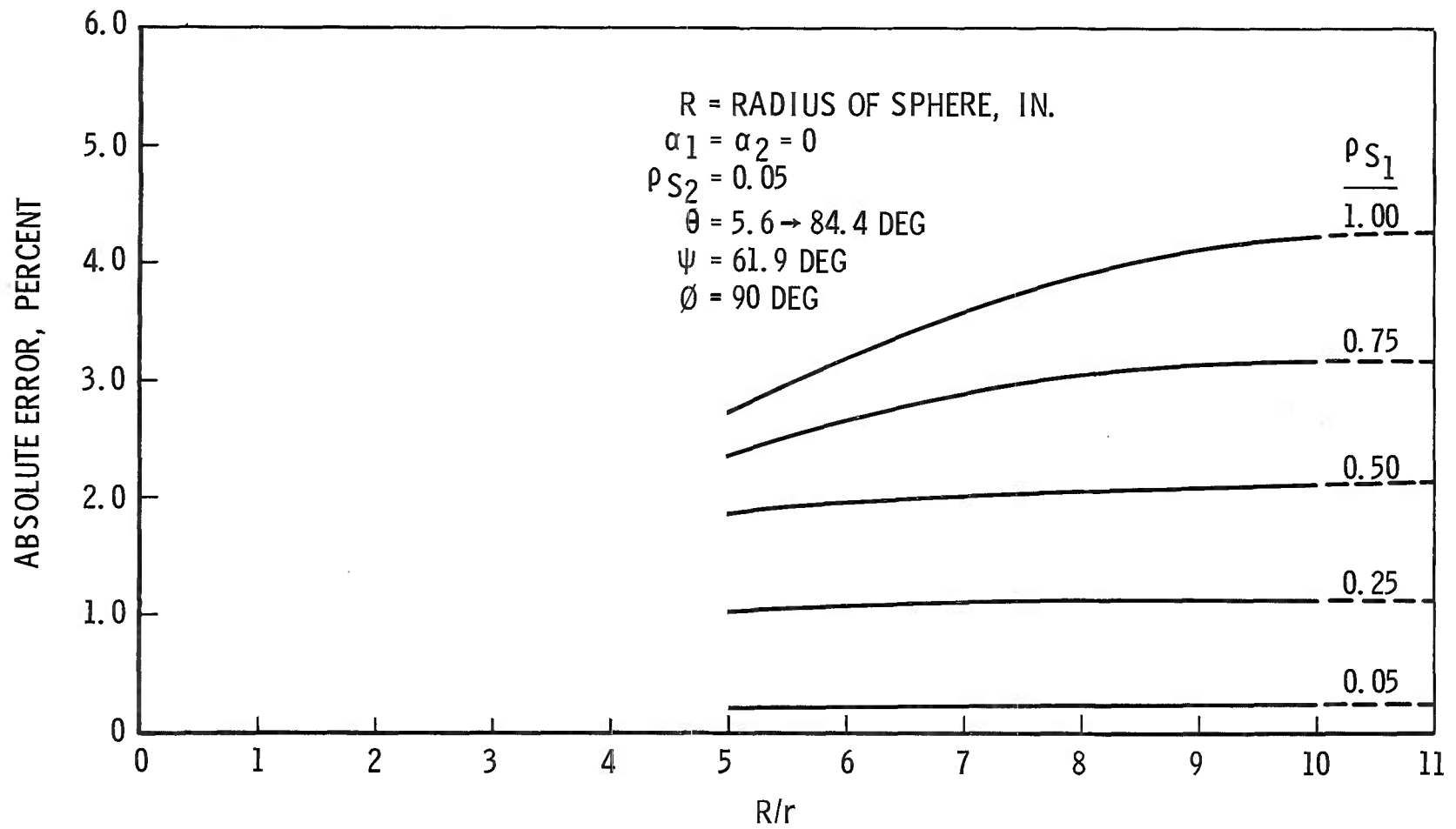
$\dfrac{\rho_{S_1}}{1.00}$

0.75

0.50

0.25

0.05

Fig. 11 Absolute Error as a Function of R/r
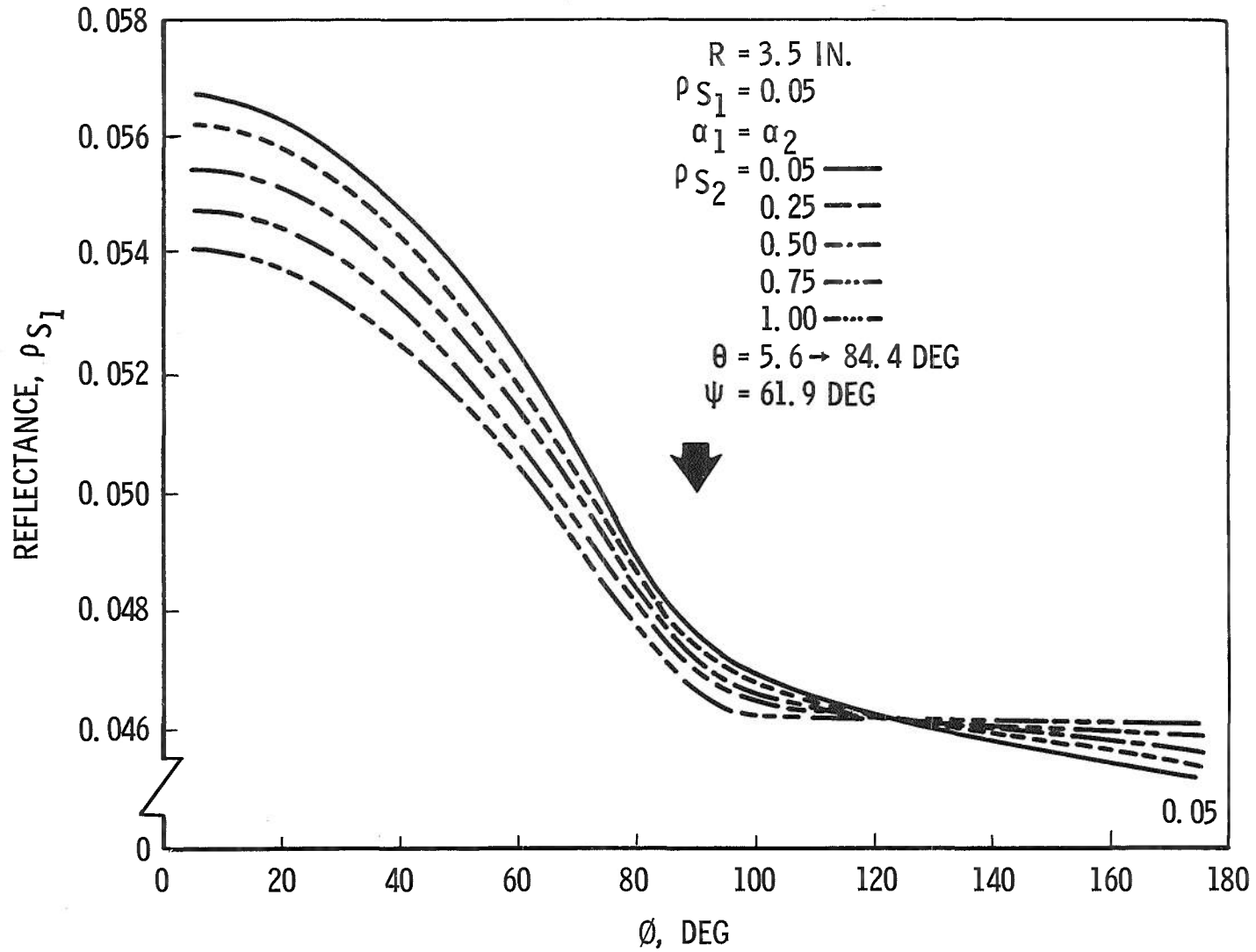
Fig. 12 Effect of ρ_{S_2} on Calculated ρ_{S_1}
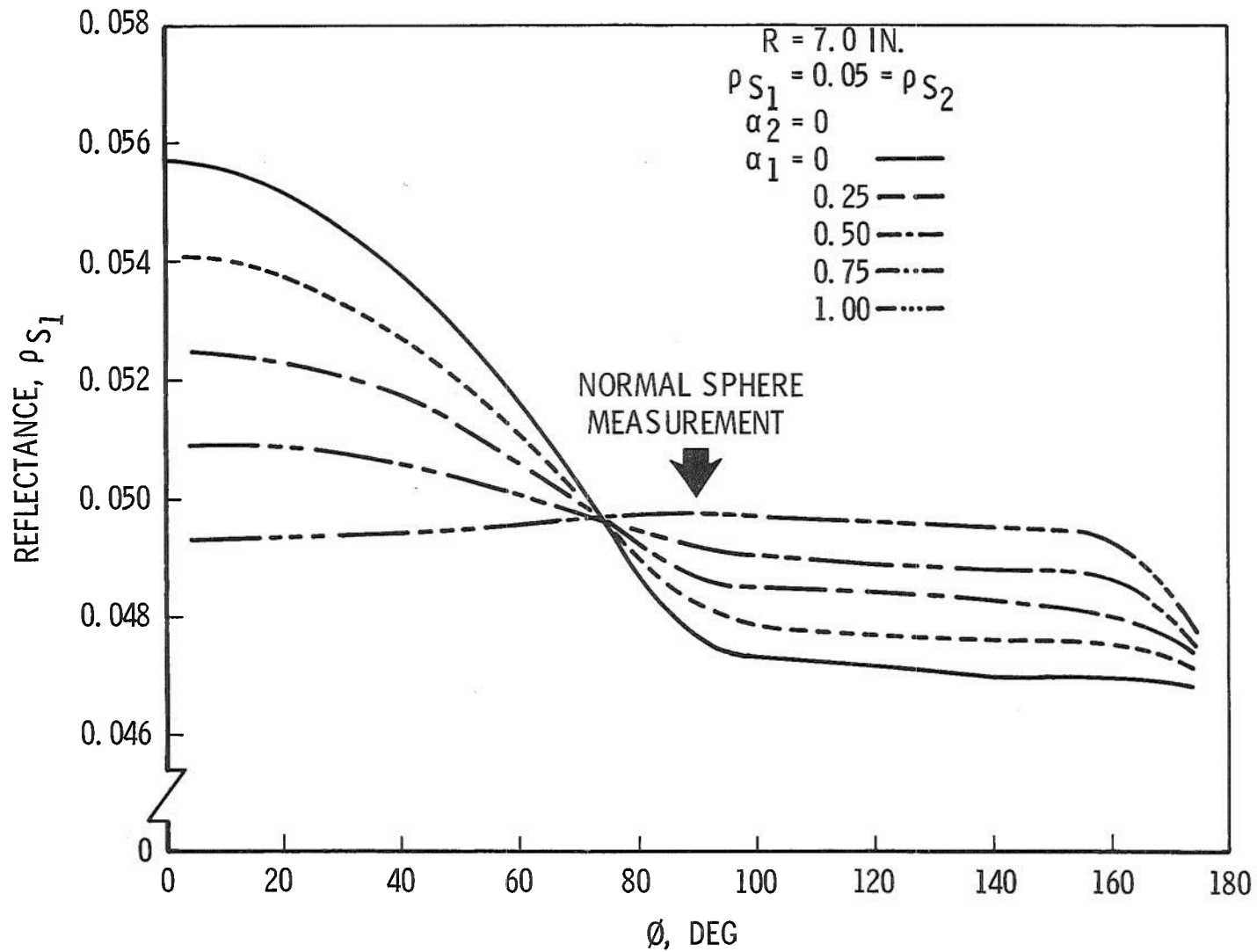
Fig. 13 Reflectance as a Function of ϕ and α,
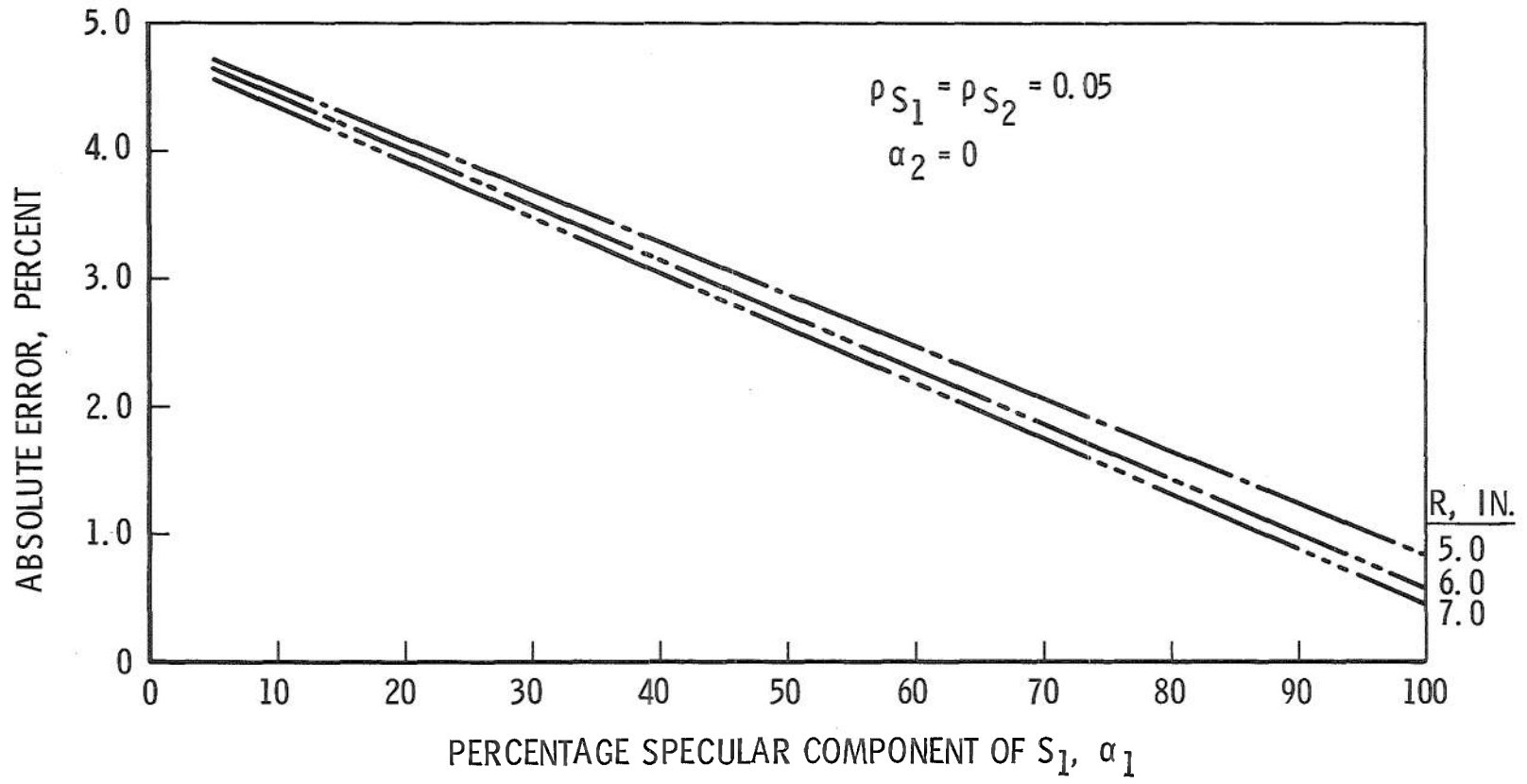
Fig. 14 Error as a Function of α_1 and R
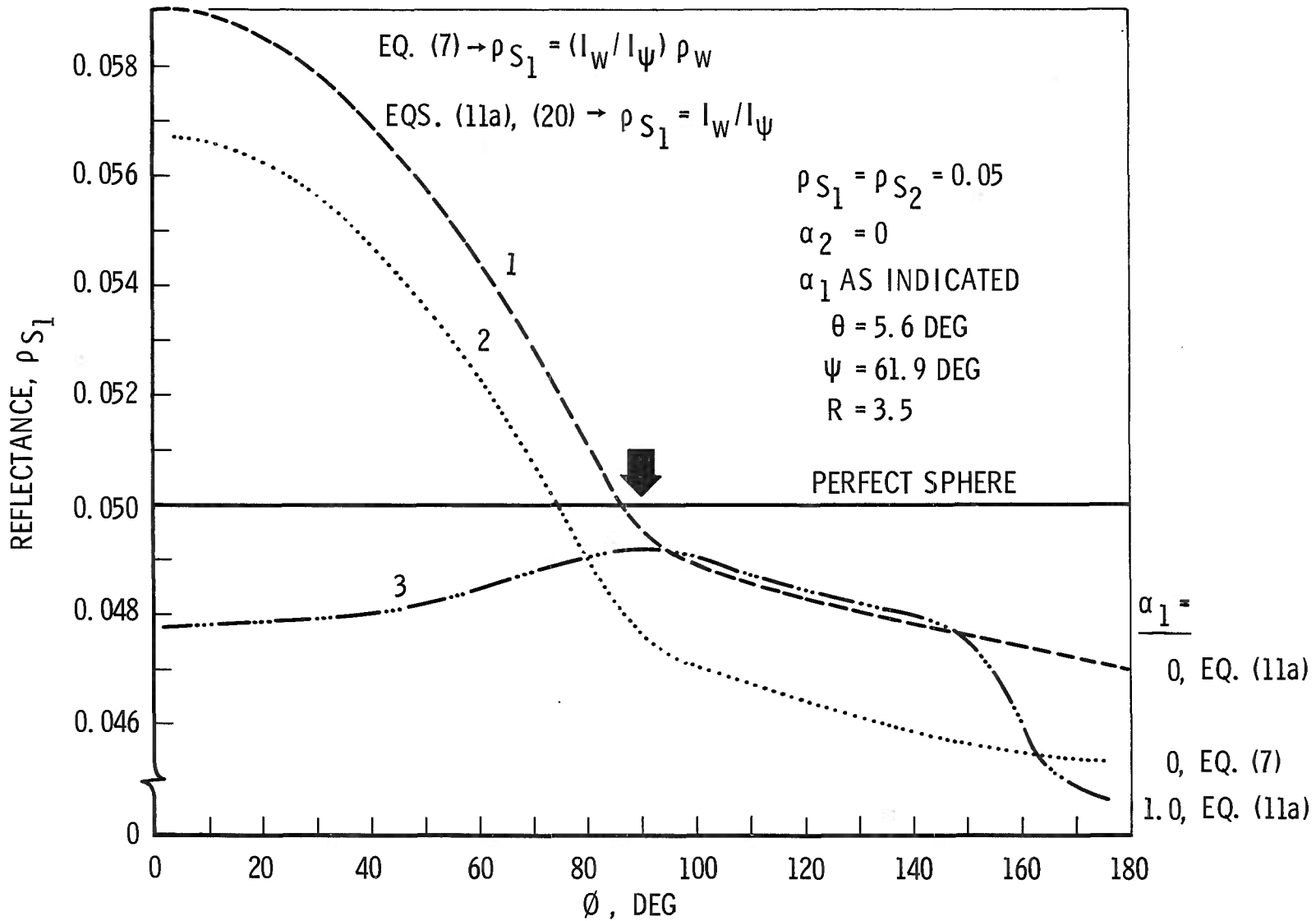
Fig. 15 Comparison of Calculation Methods

NORMAL

IRRADIATED
HEMISPHERICALLY

SURFACE IN THE
yz PLANE

ϕ

y

β

Δw_r

AZIMUTHAL
ANGLE

z
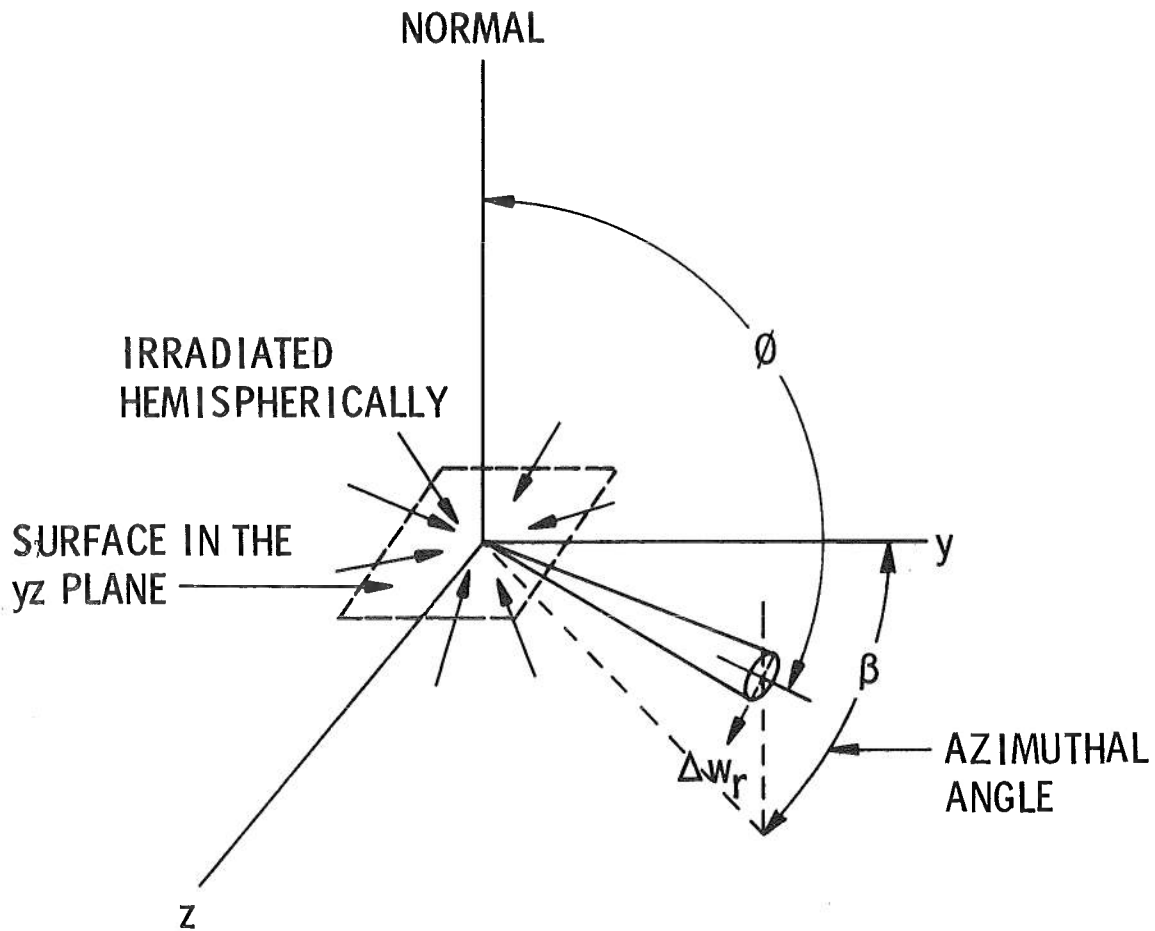
Fig. 16 Hemispherical-Angular Technique

TABLE I
ABSOLUTE ERROR IN REFLECTANCE MEASUREMENTS USING ANGULAR HEMISPHERICAL TECHNIQUE

I ρ_{S_1}	II ρ_{S_2}	III Percent Error*	IV Percent Error+	V Percent Error**	VI
0.05	0.50	0.3	0.13	0.2	Calc
0.25	0.50	1.2	0.5	0.8	Calc
0.50	0.50	2.2	0.8	1.4	Calc
0.75	0.50	3.4	0.7	1.7	Calc
1.00	0.50	3.2	0.4	1.6	Calc
0.05	0.05	0.2	0.1	0.2	Calc
0.25	0.05	1.6	0.3	0.9	Calc
1.00	0.05	2.4	0.4	1.8	Calc
0.96	0.05	2.6	0.5	2.0	Expt'l
0.96	0.96	3.1	0.2	1.9	Expt'l

* ϕ = 90 deg, θ = 5.6 deg from Eq. (7)

+ ϕ = 95 deg, θ = 5.6 deg from Eq. (11a)

** ϕ = 130 deg, θ = 5.6 deg from Eq. (11a)

DOCUMENT CONTROL DATA - R&D

(Security classification of title, body of abstract and indexing annotation must be entered when the overall report is classified)

1. ORIGINATING ACTIVITY (Corporate author)	2a. REPORT SECURITY CLASSIFICATION
Arnold Engineering Development Center (AEDC) ARO, Inc., Operating Contractor Arnold Air Force Station, Tennessee	UNCLASSIFIED
	2b. GROUP N/A

3. REPORT TITLE

DEVIATIONS FROM INTEGRATING SPHERE THEORY CAUSED BY CENTRALLY LOCATED SAMPLES

4. DESCRIPTIVE NOTES *(Type of report and inclusive dates)*

N/A

5. AUTHOR(S) *(Last name, first name, initial)*

Dawson, J. P., Todd, D. C., Wood, B. E., et al., ARO, Inc.

6. REPORT DATE	7a. TOTAL NO. OF PAGES	7b. NO. OF REFS
April 1966	42	15

8a. CONTRACT OR GRANT NO. AF40(600)-1200	9a. ORIGINATOR'S REPORT NUMBER(S)
b. PROJECT NO. 8951	AEDC-TR-65-271
c. Program Element 61445014	9b. OTHER REPORT NO(S) *(Any other numbers that may be assigned this report)* N/A
d.	

10. AVAILABILITY/LIMITATION NOTICES

Qualified requesters may obtain copies of this report from DDC. Distribution of this document is unlimited.

11. SUPPLEMENTARY NOTES	12. SPONSORING MILITARY ACTIVITY Arnold
N/A	Engineering Development Center (AEDC), Air Force Systems Command (AFSC), Arnold Air Force Station, Tennessee

13. ABSTRACT

A review of the assumptions made in the theory of the classical integrating sphere is given. The validity of these assumptions as applied to a modified integrating sphere is discussed in terms of a computer analysis and experimental data. The results of the analysis indicate that a possible error of 15 percent may be introduced into the absolute reflectance determinations. This can occur when the classical theory is applied to a modified integrating sphere using the angular-hemispherical technique. The parameters considered in the analysis are irradiance, sphere radius, sample reflectance, specular component of the sample, angle of incidence, and detector location.

DD FORM 1473
1 JAN 64

14. KEY WORDS	LINK A		LINK B		LINK C	
	ROLE	WT	ROLE	WT	ROLE	WT
integrating theory						
reflectance						
irradiance						
sphere radius						
specular components						
angle of incidence						
detectors						

INSTRUCTIONS

1. ORIGINATING ACTIVITY: Enter the name and address of the contractor, subcontractor, grantee, Department of Defense activity or other organization *(corporate author)* issuing the report.

2a. REPORT SECURITY CLASSIFICATION: Enter the over-all security classification of the report. Indicate whether "Restricted Data" is included. Marking is to be in accordance with appropriate security regulations.

2b. GROUP: Automatic downgrading is specified in DoD Directive 5200.10 and Armed Forces Industrial Manual. Enter the group number. Also, when applicable, show that optional markings have been used for Group 3 and Group 4 as authorized.

3. REPORT TITLE: Enter the complete report title in all capital letters. Titles in all cases should be unclassified. If a meaningful title cannot be selected without classification, show title classification in all capitals in parenthesis immediately following the title.

4. DESCRIPTIVE NOTES: If appropriate, enter the type of report, e.g., interim, progress, summary, annual, or final. Give the inclusive dates when a specific reporting period is covered.

5. AUTHOR(S): Enter the name(s) of author(s) as shown on or in the report. Enter last name, first name, middle initial. If military, show rank and branch of service. The name of the principal author is an absolute minimum requirement.

6. REPORT DATE: Enter the date of the report as day, month, year; or month, year. If more than one date appears on the report, use date of publication.

7a. TOTAL NUMBER OF PAGES: The total page count should follow normal pagination procedures, i.e., enter the number of pages containing information.

7b. NUMBER OF REFERENCES: Enter the total number of references cited in the report.

8a. CONTRACT OR GRANT NUMBER: If appropriate, enter the applicable number of the contract or grant under which the report was written.

8b, 8c, & 8d. PROJECT NUMBER: Enter the appropriate military department identification, such as project number, subproject number, system numbers, task number, etc.

9a. ORIGINATOR'S REPORT NUMBER(S): Enter the official report number by which the document will be identified and controlled by the originating activity. This number must be unique to this report.

9b. OTHER REPORT NUMBER(S): If the report has been assigned any other report numbers *(either by the originator or by the sponsor)*, also enter this number(s).

10. AVAILABILITY/LIMITATION NOTICES: Enter any limitations on further dissemination of the report, other than those imposed by security classification, using standard statements such as:

(1) "Qualified requesters may obtain copies of this report from DDC."

(2) "Foreign announcement and dissemination of this report by DDC is not authorized."

(3) "U. S. Government agencies may obtain copies of this report directly from DDC. Other qualified DDC users shall request through

_____ ."

(4) "U. S. military agencies may obtain copies of this report directly from DDC. Other qualified users shall request through

_____ ."

(5) "All distribution of this report is controlled. Qualified DDC users shall request through

_____ ."

If the report has been furnished to the Office of Technical Services, Department of Commerce, for sale to the public, indicate this fact and enter the price, if known.

11. SUPPLEMENTARY NOTES: Use for additional explanatory notes.

12. SPONSORING MILITARY ACTIVITY: Enter the name of the departmental project office or laboratory sponsoring *(paying for)* the research and development. Include address.

13. ABSTRACT: Enter an abstract giving a brief and factual summary of the document indicative of the report, even though it may also appear elsewhere in the body of the technical report. If additional space is required, a continuation sheet shall be attached.

It is highly desirable that the abstract of classified reports be unclassified. Each paragraph of the abstract shall end with an indication of the military security classification of the information in the paragraph, represented as *(TS)*, *(S)*, *(C)*, or *(U)*.

There is no limitation on the length of the abstract. However, the suggested length is from 150 to 225 words.

14. KEY WORDS: Key words are technically meaningful terms or short phrases that characterize a report and may be used as index entries for cataloging the report. Key words must be selected so that no security classification is required. Identifiers, such as equipment model designation, trade name, military project code name, geographic location, may be used as key words but will be followed by an indication of technical context. The assignment of links, rules, and weights is optional.